

Modified gravity interpretation of the evolving dark energy in light of DESI data

Anton Chudaykin^{1,*} and Martin Kunz^{1,†}

¹*Département de Physique Théorique and Center for Astroparticle Physics,
Université de Genève, 24 quai Ernest Ansermet, 1211 Genève 4, Switzerland*

The Dark Energy Spectroscopic Instrument (DESI) collaboration has recently released measurements of baryon acoustic oscillation (BAO) from the first year of observations. A joint analysis of DESI BAO, CMB, and SN Ia probes indicates a preference for time-evolving dark energy. We evaluate the robustness of this preference by replacing the DESI distance measurements at $z < 0.8$ with the SDSS BAO measurements in a similar redshift range. Assuming the w_0w_a CDM model, we find an evolution of the dark energy equation of state parameters consistent with Λ CDM. Our analysis of χ^2 statistics across various BAO datasets shows that DESI's preference for evolving dark energy is primarily driven by the two LRG samples at $z_{\text{eff}} = 0.51$ and $z_{\text{eff}} = 0.71$, with the latter having the most significant impact.

Taking this preference seriously, we study a general Horndeski scalar-tensor theory, which provides a physical mechanism to safely cross the phantom divide, $w = -1$. Utilizing the Effective Field Theory of dark energy and adopting the w_0w_a CDM background cosmological model, we derive constraints on the parameters $w_0 = -0.856 \pm 0.062$ and $w_a = -0.53^{+0.28}_{-0.26}$ at 68% CL from Planck CMB, Planck and ACT CMB lensing, DESI BAO, and Pantheon+ datasets, showing good consistency with the standard w_0w_a CDM model. The modified gravity model shows a preference over Λ CDM at the 2.4σ level, while for w_0w_a CDM it is at 2.5σ . We conclude that modified gravity offers a viable physical explanation for DESI's preference for evolving dark energy.

I. INTRODUCTION

Recent measurements of baryon acoustic oscillations (BAO) from the first year of observations from the Dark Energy Spectroscopic Instrument (DESI) find hints towards a time-evolving equation of state of dark energy [1]. The BAO measurements have been obtained in seven redshift bins using galaxy, quasar, and Lyman- α forest tracers across $0.1 < z < 4.2$. They are expressed in terms of the transverse comoving distance D_M/r_d , the Hubble distance, D_M/r_d , or their combination, the angle-averaged distance D_V/r_d , normalized to the comoving sound horizon at the end of baryon drag epoch. While the DESI BAO data alone are consistent with the standard Λ CDM model, the combination with external datasets yield results discrepant with the concordance cosmological scenario.

Allowing for a time-varying dark energy equation of state, parameterized by $w(a) = w_0 + w_a(1 - a)$, combinations of DESI with cosmic microwave background (CMB) or type Ia supernovae measurements individually favours $w_0 > -1$ and $w_a < 0$. This preference is 2.6σ for the DESI+CMB data, and increases when adding supernova measurements. A joint analysis of DESI, CMB, and SN Ia probes gives results discrepant with the Λ CDM model at the 2.5σ , 3.5σ and 3.9σ levels when using Pantheon+ [2], Union3 [3], or Dark Energy Survey (DES) Y5 [4] supernova datasets, respectively.

The DESI collaboration reported systematically larger observed BAO scales than the prediction of Planck 2018

Λ CDM cosmology at $z < 0.8$, and therefore lower distances. For LRG1 at $z_{\text{eff}} = 0.51$, the DESI data prefers a mildly larger line-of-sight BAO scale compared to the transverse scale, leading to a smaller D_H/D_M compared than the Planck Λ CDM prediction. For LRG2 at $z_{\text{eff}} = 0.71$, the discrepancy is sourced from the transverse BAO scale, implying a smaller D_M/r_d and D_V/r_d at this redshift. Accordingly, DESI reported an approximate 3σ discrepancy between the DESI BAO measurement at $z_{\text{eff}} = 0.71$ and the SDSS measurement at $z_{\text{eff}} = 0.7$ [1].¹ Given the consistency of the DESI measurements with SDSS at $z > 0.8$ [7], the difference between the two BAO datasets originates solely from $z < 0.8$. This observation suggests an important consistency check of the DESI results, which involves replacing the low-redshift DESI data at $z < 0.8$ with the SDSS BAO measurements.

The DESI collaboration performed a consistency test by replacing the data at $z < 0.6$ with SDSS while using a combined “DESI+SDSS” BAO dataset at $z > 0.6$. This test showed a good agreement with the baseline analysis that utilized the entire DESI data. Notably, the constraints in the w_0 - w_a plane shifted closer to the Λ CDM expectation, and the significance of the tension with Λ CDM marginally decreased to 2.1σ with the Pantheon+ data [1]. Crucially, this test retained the $z_{\text{eff}} = 0.71$ DESI point, which shows the greatest discrepancy with both the Planck Λ CDM expansion history and the SDSS distance measurement at $z_{\text{eff}} = 0.71$. Given the previous studies [7, 8] suggesting a significant role of the LRG2 in driving the DESI preference for the w_0w_a -model relative

* anton.chudaykin@unige.ch

† martin.kunz@unige.ch

¹ The SDSS catalog at $z_{\text{eff}} = 0.7$ is a composite dataset formed from the BOSS CMASS galaxy sample and the eBOSS LRG sample, for details see [5, 6].

to Λ CDM, replacing this point with the SDSS data is capable of reducing the evidence for time-evolving dark energy as we will show in Section III A below.

One particular aspect of the preference of the DESI+CMB+SN data for an evolving dark energy equation of state is that the preferred models cross the ‘phantom divide’, $w = -1$, which was also noticed by the DESI collaboration [9]. To some extent this is driven by the CMB data, which fixes the distance to last scattering to be close to the Λ CDM expectation, which requires to compensate a positive $1 + w$ at low redshift with a negative value at higher redshift [10]. This adds an additional challenge when trying to interpret the DESI results in terms of physical models. The w_0w_a -model offers a phenomenological description of the equation of state of dark energy at the background level, but it fails to provide a satisfactory description for dark energy perturbations. The dark energy perturbations are usually taken to be those of an canonical minimally-coupled scalar field component, but this model lacks a physical mechanism to safely cross the phantom divide. To avoid singularities in the fluid equation of motion, one commonly employs the parameterized post-Friedman approach to metric perturbations [11]. Although this framework is extensively used in the literature, it provides only an effective prescription of the perturbation evolution and is not based on a full physical model. Hence, a physical model for dark energy perturbations is necessary.

The phantom crossing in the dark energy equation of state can be naturally realized in models involving multiple scalar fields, alternative models of gravity with Kinetic Gravity Braiding, or with non-minimal couplings. For the purposes of this analysis, we consider a Horndeski theory of gravity with an additional scalar degree of freedom, which features at most second-order derivatives in the equations of motion. This class of theories is quite general and encompasses a large groups of popular dark energy and modified gravity models, including $f(R)$ gravity, Brans-Dicke theory, quintessence, k-essence, Galileons, and many other more exotic possibilities and combinations, some of which can cross the phantom divide self-consistently. Given the extensive landscape of modified gravity theories, it is beneficial to use a flexible framework that allows for a model-independent description of the effects of modified gravity.

An efficient and systematic description of the linear perturbations in a general Horndeski theory is provided by the Effective Field Theory (EFT) of dark energy. In this approach, all the possible modifications of the Einstein-Hilbert action, which govern the evolution of linear perturbations, are parameterized by a set of fixed operators that respect the symmetries of the cosmological background in unitary gauge. The contribution of each operator is controlled by EFT coefficients, which are functions of time only and are often referred to as “ α -functions”. On the EFT grounds, the α -functions are arbitrary functions of time. However, current astrophysical data is not sufficiently constraining for general func-

tions. Consequently, a common approach is to assume specific parametrizations for the α -functions, thereby reducing their time-dependence to a set of well-defined parameters. Constraints on these parameters serve as a test for deviations from General Relativity in a largely model-independent manner. Another advantage of the EFT-based approach is that the background expansion is entirely independent of the dynamics of linear perturbations, offering a more flexible framework for testing non-GR effects at the perturbative level.

In this work, we investigate the preference for a dynamical dark energy from the DESI BAO DR1 data in combination with external datasets including Planck CMB, Planck+ACT CMB lensing, DESI and SDSS BAO measurements, and the Pantheon+ supernova sample. First, we identify the source of this preference in the DESI data assuming the w_0w_a CDM model. Second, we evaluate the robustness of these results by replacing the low-redshift DESI BAO data with the SDSS measurements. Third, we evaluate parameter estimates within a general Horndeski theory, allowing for a reasonable degree of freedom in the dynamics of linear perturbations within the EFT of dark energy approach. For the sake of comparison with the w_0w_a CDM scenario, we set the background cosmological model to w_0w_a CDM.

Our paper is structured as follows. We describe the analysis procedure and data in Sec. II. Our final results are presented in Sec. III. We draw conclusions in Sec. IV.

II. ANALYSIS PROCEDURE

We investigate dark energy dynamics with the w_0w_a CDM model and the general scalar-tensor Horndeski theory. In w_0w_a CDM, we utilize the standard parametrization for the dark energy equation of state, given by $w(a) = w_0 + w_a(1-a)$. For Horndeski gravity, we adopt a model-independent parametrization based on the Effective Field Theory (EFT) of dark energy. Hereafter, we will refer to this modified gravity model as “MG”.

A. EFT of dark energy

In the EFT-based approach to modified gravity, the dynamics of linear perturbations associated with a scalar degree of freedom is parameterized by four arbitrary functions of time, termed α -functions. These include the kineticity parameter α_K , which modulates the kinetic term for scalar field perturbations, the braiding parameter α_B , which controls a mixing between the kinetic terms of the metric and the scalar field, the running of the effective Planck mass α_M , and the tensor speed excess α_T , which captures the difference between the propagation

speed of gravitational waves and the speed of light.²

In order to extract meaningful cosmological constraints within the EFT-based framework, it is necessary to specify a parametrization for the α -functions. We set the time-dependence of the α -functions to match the density fraction of dark energy, $\alpha_i(a) = c_i \Omega_{DE}(a)$, where c_i is a free constant parameter. This parametrization ensures that $\alpha_i \rightarrow 0$ at early time, consistent with the expectation that any modifications of gravity are suppressed during epochs when dark energy does not significantly contribute to the energy density of the Universe. Additionally, as mentioned, we assume a $w_0 w_a$ CDM background cosmology.

The general form of the $\alpha_i(a)$ and the background expansion $H(a)$ within the EFT-based framework can lead to ill-defined theories. To prevent pathological behavior, we enforce several stability conditions that guarantee the absence of ghost and gradient instabilities, as implemented in `hi_class` [13]. Tachyon instabilities are considered less pathological, since they appear in the low- k limit, and come under control when the mode enters the sound horizon (see [14] and references therein). Therefore, we adopt a conservative approach and do not impose the no-tachyon condition, allowing the data to exclude such scenarios.

B. Methodology

Parameter estimates in this paper are obtained with the publicly available code `hi_class` [13, 15], interfaced with the `Montepython` Monte Carlo sampler. `hi_class` is an extension of the Boltzmann code `CLASS` [16] and calculates the evolution of linear cosmological perturbations for general Horndeski scalar-tensor gravity theories. Modified gravity models can be specified either within the Effective Field Theory of Dark Energy approach or through the full covariant action. In this work, we utilize the EFT-based parameterized approach.

We perform Markov chain Monte Carlo (MCMC) analyses to sample the posterior distributions using the Metropolis-Hastings algorithm. We adopt a Gelman-Rubin [17] convergence criterion $R - 1 < 0.02$, except in the MG model, where we require a still sufficient threshold of $R - 1 < 0.1$ (unless otherwise stated) due to the higher computational cost. The plots and marginalized constraints are generated with the publicly available `getdist` package.³

In the minimal Λ CDM model we vary 6 standard cosmological parameters within broad uniform priors:

$\omega_{cdm} = \Omega_c h^2$, $\omega_b = \Omega_b h^2$, H_0 , $\ln(10^{10} A_s)$, n_s and τ . In the $w_0 w_a$ CDM scenario we sample two additional parameters, (w_0, w_a) , which parameterize a time-varying equation of state for dark energy. We adopt the uniform priors on the dark energy parameters, $w_0 \in [-3, 1]$ and $w_a \in [-3, 2]$, as specified in [1]. Since we explore the parameter space that allows the dark energy equation of state to cross the $w = -1$ boundary, we use the parameterized post-Friedman approach [11] to compute dark energy perturbations in the $w_0 w_a$ CDM scenario. Additionally, we impose the condition $w_0 + w_a < 0$, ensuring a matter domination stage in the past. In Horndeski theory, we additionally vary two EFT amplitudes, c_B and c_M , within broad uniform priors while fixing $c_K = 1$. We also set $c_T = 0$ to address the tight constraint on the speed of propagation of gravitational waves. In all cases, we assume a spatially flat universe with two massless and one massive neutrino species with $m_\nu = 0.06$ eV. In the Λ CDM and $w_0 w_a$ CDM models, we use the `Halofit` module to compute the non-linear matter power spectrum, whereas in general Horndeski theory only the linear prediction is utilized.

In our analyses we compute the best-fit predictions as follows. We perform an additional MCMC by multiplying the log-posteriors by a factor 100 and rescaling the covariance of the proposal distribution by a factor of 0.01. This approach enhances the efficiency of sampling in the high probability region, thereby improving the precision of the best-fit model recovery. We assess the uncertainty in the calculation of the minimum χ^2 to be 0.2 by performing 10 independent minimizations. This level of accuracy is sufficient to reach robust conclusions.

C. Data

We consider the following datasets in our MCMC analyses:

1. CMB

We employ the official Planck high- ℓ `plik` TT,TE,EE likelihood, together with low- ℓ TT `Commander` and EE `SimAll` likelihoods [18]. In addition to the primary CMB anisotropy, we include the measurement of the lensing potential power spectrum, $C_\ell^{r\phi\phi}$, from the combination of NPIPE PR4 Planck CMB maps [19] and the Data Release 6 of the Atacama Cosmology Telescope (ACT) [20].⁴ We will refer to the CMB data simply as ‘‘CMB’’.

Recently, a new Planck data release, PR4, has been made available, involving a reprocessing of the data from

² We set the effective Planck mass at early times to be M_{Pl} , since we focus on late-time modifications of gravity and do not aim to simultaneously constrain early-time modifications. The initial value of the effective Planck mass is tightly constrained by CMB data [12].

³ <https://getdist.readthedocs.io/en/latest/>

⁴ The likelihood is publicly available at https://github.com/ACTCollaboration/act_dr6_lenslike; we use `actplanck.baseline` option.

TABLE I. BAO measurements used in our analysis along with their tags, effective redshift, and number of data points. The upper group contains the DESI BAO data [1], while the bottom group refers to the SDSS BAO measurements [5].

Data	z_{eff}	N_{data}
BGS	0.30	1
LRG1	0.51	2
LRG2	0.71	2
LRG3+ELG1	0.93	2
ELG2	1.32	2
QSO	1.49	1
Lya	2.33	2
MGS	0.15	1
BOSS DR12	0.38 and 0.51	4
eBOSS DR16	0.7	2

both the LFI and HFI channels with the latest and most accurate pipeline, NPIPE [21]. This release features lower levels of noise and systematics, as well as slightly more data. In our analysis, we use the official PR3 `plik` likelihood for the following reasons. First, shifts in parameter estimates inferred from the PR3 and PR4 Planck likelihoods become non-significant after combining with CMB lensing likelihoods from Planck and ACT. Second, we retain `plik` as our baseline to closely align with the DESI analysis.

2. BAO

In our baseline analysis we utilize the DESI DR1 BAO data as specified in Tab. I of Ref. [1], which consists of the BSG sample in the redshift range $0.1 < z < 0.4$, LRG1 and LRG2 samples in $0.4 < z < 0.6$ and $0.6 < z < 0.8$, combined LRG3+ELG1 sample in $0.8 < z < 1.1$, ELG2 sample in $1.1 < z < 1.6$, quasar sample in $0.8 < z < 2.1$ and Lyman- α Forest sample spanning $1.77 < z < 4.16$. We will refer to this BAO data as “DESI BAO”.

To explore the effect of low-redshift BAO measurements, we construct a combined dataset which comprises SDSS BAO data in the low-redshift region $z < 0.8$ and DESI BAO data in high-redshift region $z > 0.8$. In particular, we adopt the SDSS BAO distance measurements extracted from DR7 Main Galaxy Sample (MGS) [22] in $0.07 < z < 0.2$, BOSS DR12 galaxy samples in $0.2 < z < 0.5$ and $0.4 < z < 0.6$ [23], eBOSS DR16 galaxy sample in $0.6 < z < 1.0$ [5] in place of the DESI BGS, LRG1 and LRG2 points. We use the label “DESI+SDSS” to refer to this composite dataset.

We summarize the BAO measurements used in this work in Tab. I.

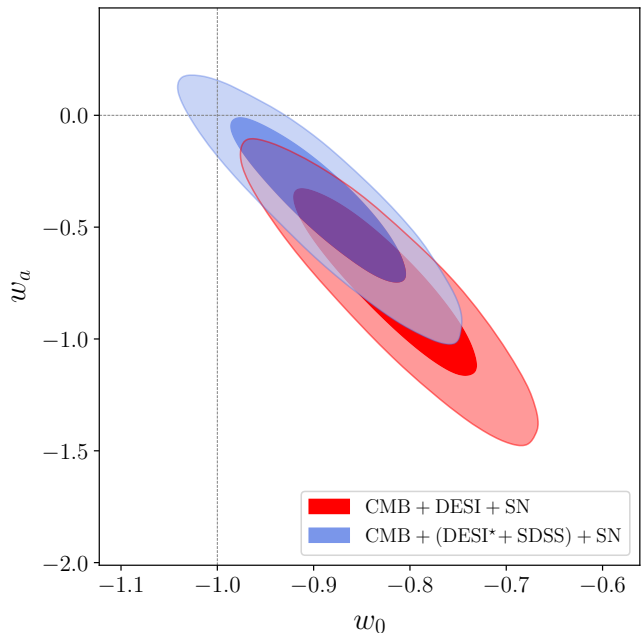


FIG. 1. 68% and 95% marginalized posterior constraints in the $w_0 - w_a$ plane for the $w_0 w_a$ CDM model from CMB + DESI + SN (red) and CMB + (DESI* + SDSS) + SN (blue) datasets.

3. SN

We utilize supernova data from the Pantheon+ sample [2], which consists of 1550 spectroscopically confirmed SNe I in the redshift range $0.001 < z < 2.26$. We do not apply any external calibration from astrophysical measurements and allow a supernova absolute magnitude to vary freely. We adopt the `PantheonPlus` likelihood in `MontePython` and recall this dataset as “SN” in what follows.

III. RESULTS AND DISCUSSIONS

A. $w_0 w_a$ CDM model

In this section, we explore a time-varying dark energy equation of state, $w(a) = w_0 + w_a(1 - a)$, referred to as $w_0 w_a$ CDM.

Fig. 1 presents the marginalized constraints in the $w_0 - w_a$ plane from different data. We start by analyzing cosmological constraints from the CMB + DESI + SN combination utilized in the official DESI analysis. The resulting 68% credible-interval constraints are

$$\left. \begin{aligned} w_0 &= -0.821 \pm 0.065, \\ w_a &= -0.76^{+0.31}_{-0.26}, \end{aligned} \right\} \text{CMB+DESI+SN} \quad (1)$$

Our parameter estimates align closely with the results of the official DESI analysis. The minimum $\Delta\chi^2$ value

sume that this evidence is real and utilize the entire set of DESI distance measurements in what follows.

B. MG model

We now explore a general Horndeski scalar-tensor theory that in principle allows the dark energy equation of state to evolve across the phantom divide, $w = -1$. First of all, we found that our results are not sensitive to the kineticity parameter α_K . This is expected, since α_K has minimal impact on sub-horizon physics [26, 27]. For definiteness, we fix $\alpha_K = 1$ in our analysis.

Fig. 3 shows the posterior distributions in the $w_0 - w_a - \alpha_B - \alpha_M$ space for the MG model. The one-dimensional parameter constraints are

$$\left. \begin{aligned} w_0 &= -0.856 \pm 0.062, \\ w_a &= -0.53^{+0.28}_{-0.26}, \\ \alpha_B &= 0.82^{+0.31}_{-0.46}, \\ \alpha_M &= 0.88^{+0.75}_{-1.28}. \end{aligned} \right\} \text{CMB+DESI+SN} \quad (3)$$

Full parameter estimates from various datasets are provided in App. A.

The MG model offers a satisfactory physical description of time-evolving dark energy, allowing for the crossing of the phantom divide, $w = -1$. In particular, the w_0 posterior deviates from -1 at the 2.4σ level. The minimum $\Delta\chi^2$ value between the MG model and the concordance cosmology is -12.2 for 4 additional degrees of freedom. This reflects a slightly lower preference for evolving dark energy at the 2.4σ level when compared to the w_0w_a CDM scenario.

Constraints on the MG parameters are primarily driven by the late integrated Sachs-Wolfe (ISW) effect. The ISW effect especially excludes cosmologies with large α_B and α_M values, as it leads to a large excess of power in the TT CMB power spectrum on large scales [13]. For not very large c_i , the effect of modified gravity conspires to prevent large power in the TT CMB power spectrum, resulting in the particular degeneracy directions in the $\alpha_M - \alpha_B$ plane [27]. The data shows a mild preference for positive values of the braiding parameter, $\alpha_B > 0.11$ at 95% CL., in agreement with the previous study [27]. The lower boundary for α_M is driven by the onset of gradient instabilities.

While $\alpha_M = 0$ provides a good fit to the data, non-minimal coupling play an important role in the MG constraints. For the scalar minimally coupled to gravity ($\alpha_M = 0$), the region $\alpha_B < 0.4$ is excluded due to the presence of gradient instabilities. A non-zero α_M shifts the gradient stability condition, making cosmologies with small α_B viable. The region of small α_B is then disfavoured by the data, as it implies too large α_M , which leads to large power in the C_ℓ^{TT} via the late-time ISW effect. Thus, non-minimal coupling provides more flexibility, enabling the data to explore the full parameter space in the MG scenario.

TABLE II. $\Delta\chi^2_{\text{model}} \equiv \chi^2_{\text{model}} - \chi^2_{\Lambda\text{CDM}}$ values for the different best-fit models optimized to the CMB+DESI+SN data. The minimum χ^2 values were obtained using the Halofit non-linear matter power spectrum, see discussion in the text.

Data	$\Delta\chi^2_{w_0w_a}$	$\Delta\chi^2_{\text{MG}}$
CMB	-2.9	-5.9
DESI	-3.8	-4.0
SN	-2.1	-2.3
Total	-8.8	-12.2

It is important to note that measurements of the late-time fluctuation amplitude significantly improves the MG constraints by breaking the degeneracy directions in the $\alpha_M - \alpha_B$ plane, as discussed in [27]. In this work, our primary goal is to demonstrate a proof-of-principle theory that accommodates the crossing of the phantom divide, evidenced by the CMB+DESI+SN data. To streamline the analysis, we focus here on the distance measurements. We leave a detailed analysis of the MG scenario with all available data to future work.

C. Comparison And Discussion

Here, we compare the w_0w_a CDM and MG models for the CMB+DESI+SN dataset. Results for other datasets are available in App. A.

Fig. 4 shows the posterior distributions in the $w_0 - w_a$ plane for the w_0w_a CDM and MG models.

The MG scenario shows a slightly weaker preference for evolving dark energy, as evidenced by the w_0 and w_a posteriors shifting towards Λ CDM. This behaviour is mainly attributed to the CMB degeneracies between the dark energy parameters and α_B shown in Fig. 3. However, the results from the MG and w_0w_a CDM models are fully compatible.

We also compare the goodness-of-fit for different datasets between the w_0w_a CDM and MG models relative to Λ CDM. Tab. II presents the $\Delta\chi^2$ for various datasets in the CMB+DESI+SN analysis. We found that non-linear corrections to the matter power spectrum are important when calculating the minimum χ^2 . Specifically, non-linear effects significantly increase the power of the lensing potential power spectrum at small angular scales, which, if not included, worsens the fit to the CMB lensing data. To ensure a meaningful comparison, we utilize the Halofit prescription for the non-linear matter power spectrum for both models. It is important to note that the Halofit fitting formula was calibrated against Λ CDM and therefore is not expected to accurately capture the non-linear behavior of the matter power spectrum for modified gravity. Note that the w_0w_a CDM model has two additional parameters compared to Λ CDM, whereas the MG model has four extra parameters.

Both models yield nearly the same goodness-of-fit for

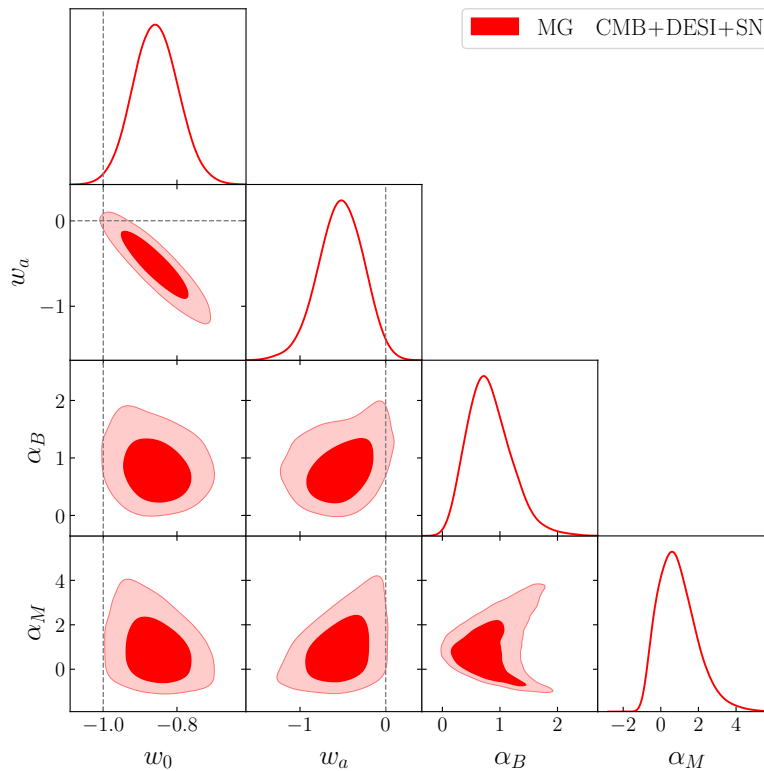


FIG. 3. 68% and 95% marginalized constraints on w_0 , w_a , α_B and α_M from the CMB+DESI+SN data in the MG model.

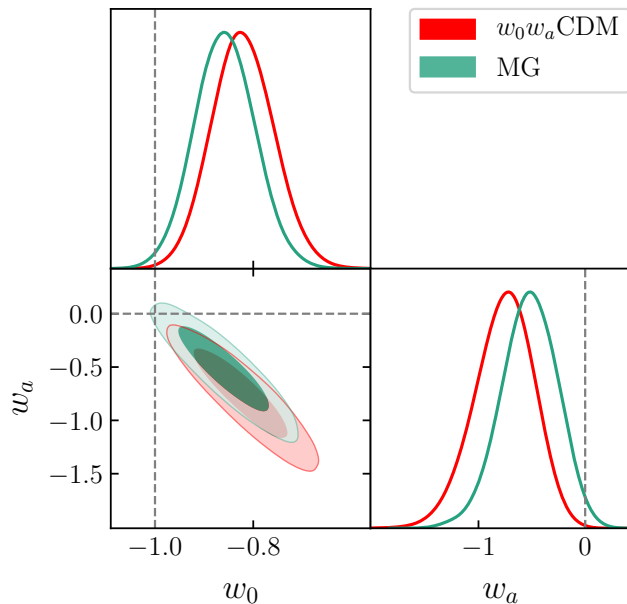


FIG. 4. 68% and 95% marginalized constraints on w_0 and w_a from the CMB+DESI+SN data in $w_0 w_a$ CDM (red) and MG (green) models.

the DESI and SN data. The MG scenario shows a better fit to the CMB, but this preference is not statistically

significant given the different number of model parameters. Although the MG scenario improves the overall χ^2 , it shows a similar preference over Λ CDM: 2.4σ for the MG model versus 2.5σ for the $w_0 w_a$ CDM model. We conclude that the MG model provides a successful physical explanation for DESI's preference for evolving dark energy.

IV. CONCLUSIONS

In this work we have explored the preference for a time-evolving dark energy in the light of the DESI DR1 BAO data. We pinpoint the source of this preference in the $w_0 w_a$ CDM model to be due to the the DESI luminous red galaxy samples at $z_{\text{eff}} = 0.51$ and $z_{\text{eff}} = 0.71$, with the latter contributing the most. We showed that replacing the DESI BAO data at $z < 0.8$ with the SDSS measurements in the corresponding redshift range diminishes this preference, making the evolution of dark energy equation of state parameter consistent with Λ CDM. We stress that definitive conclusion from the DESI preference can only be drawn when more data from the DESI DR3 release or from other ongoing and upcoming large surveys will be available.

Taking this preference seriously, we study a physical model which can explain DESI's preference for evolving dark energy in both background and perturbation dy-

namics. We explore a general Horndeski scalar-tensor gravity theory, which allows the dark energy equation of state to evolve across the phantom divide, $w = -1$. Utilizing the EFT-based framework, which offers a largely model-independent description of modified gravity effects, we derive constraints for w_0 and w_a parameters, showing good consistency with the w_0w_a CDM model. The modified gravity model indicates a preference over Λ CDM at the 2.4σ level. We conclude that modified gravity offers a viable physical explanation for DESI's preference for evolving dark energy.

It is important to investigate the robustness of our results with respect to the choice of parameterization of the α -functions. Strictly speaking, the results obtained in this work are valid only for specific subclasses of Horndeski theory where the time evolution of the α -functions is proportional to the time evolution of dark energy density in the w_0w_a background. The primary goal is to extract generic conclusions that are independent of the choice of parametrisation, see e.g. [27]. We leave a detailed study of parameterization-independent features of the constraints for future work.

Another interesting future avenue is to explore physical modified gravity models based on the full covariant action. Although this approach offers less generality than the EFT, it allows to directly relate fundamental parameters of the theory to the observational constraints. In the covariant approach, the cosmological background and the linear evolution of dark energy perturbations are determined by the same theory parameters that appear in the action, while in the EFT approach used here, the

link between the model parameters and the action is less obvious. This tends to impose a ‘simplicity constraint’ on models specified through a covariant action that often leads to tighter constraints compared to the EFT-based framework. However, the most important future development remains the arrival of new data that may or may not increase the evidence for a departure from Λ CDM.

ACKNOWLEDGMENTS

We are grateful to Emilio Bellini for fruitful discussions.

Appendix A: Full Parameter Constraints

In this appendix, we present the full parameter constraints in the MG model. Fig. 5 shows the posterior distributions on cosmological parameters from the CMB, CMB+DESI and CMB+DESI+SN datasets. The corresponding parameter constraints are listed in Tab. III.

Fig. 5 illustrates the degeneracies between various parameters present in the CMB data. The DESI distance measurements significantly improve constraints on the Λ CDM parameters, although the degeneracies among the w_0 , w_a , and other parameters persist. The addition of SN Ia data completely breaks the degeneracy in the $w_0 - w_a$ plane, thereby refining the estimates of other parameters.

-
- [1] DESI collaboration, A. G. Adame et al., *DESI 2024 VI: Cosmological Constraints from the Measurements of Baryon Acoustic Oscillations*, 2404.03002.
- [2] D. Scolnic et al., *The Pantheon+ Analysis: The Full Data Set and Light-curve Release*, *Astrophys. J.* **938** (2022) 113 [2112.03863].
- [3] D. Rubin et al., *Union Through UNITY: Cosmology with 2,000 SNe Using a Unified Bayesian Framework*, 2311.12098.
- [4] DES collaboration, T. M. C. Abbott et al., *The Dark Energy Survey: Cosmology Results With ~ 1500 New High-redshift Type Ia Supernovae Using The Full 5-year Dataset*, 2401.02929.
- [5] EBOSS collaboration, S. Alam et al., *Completed SDSS-IV extended Baryon Oscillation Spectroscopic Survey: Cosmological implications from two decades of spectroscopic surveys at the Apache Point Observatory*, *Phys. Rev. D* **103** (2021) 083533 [2007.08991].
- [6] EBOSS collaboration, A. J. Ross et al., *The Completed SDSS-IV extended Baryon Oscillation Spectroscopic Survey: Large-scale structure catalogues for cosmological analysis*, *Mon. Not. Roy. Astron. Soc.* **498** (2020) 2354 [2007.09000].
- [7] DESI collaboration, A. G. Adame et al., *DESI 2024 III: Baryon Acoustic Oscillations from Galaxies and Quasars*, 2404.03000.
- [8] Z. Wang, S. Lin, Z. Ding and B. Hu, *The role of LRG1 and LRG2's monopole in inferring the DESI 2024 BAO cosmology*, 2405.02168.
- [9] DESI collaboration, K. Lodha et al., *DESI 2024: Constraints on Physics-Focused Aspects of Dark Energy using DESI DR1 BAO Data*, 2405.13588.
- [10] E. V. Linder, *The Mirage of $w=-1$* , 0708.0024.
- [11] W. Fang, W. Hu and A. Lewis, *Crossing the Phantom Divide with Parameterized Post-Friedmann Dark Energy*, *Phys. Rev. D* **78** (2008) 087303 [0808.3125].
- [12] E. Bellini, A. J. Cuesta, R. Jimenez and L. Verde, *Constraints on deviations from Λ CDM within Horndeski gravity*, *JCAP* **02** (2016) 053 [1509.07816].
- [13] M. Zumalacárregui, E. Bellini, I. Sawicki, J. Lesgourgues and P. G. Ferreira, *hi-class: Horndeski in the Cosmic Linear Anisotropy Solving System*, *JCAP* **08** (2017) 019 [1605.06102].
- [14] N. Frusciante, G. Papadomanolakis, S. Peirone and A. Silvestri, *The role of the tachyonic instability in Horndeski gravity*, *JCAP* **02** (2019) 029 [1810.03461].
- [15] E. Bellini, I. Sawicki and M. Zumalacárregui, *hi-class: Background Evolution, Initial Conditions and*

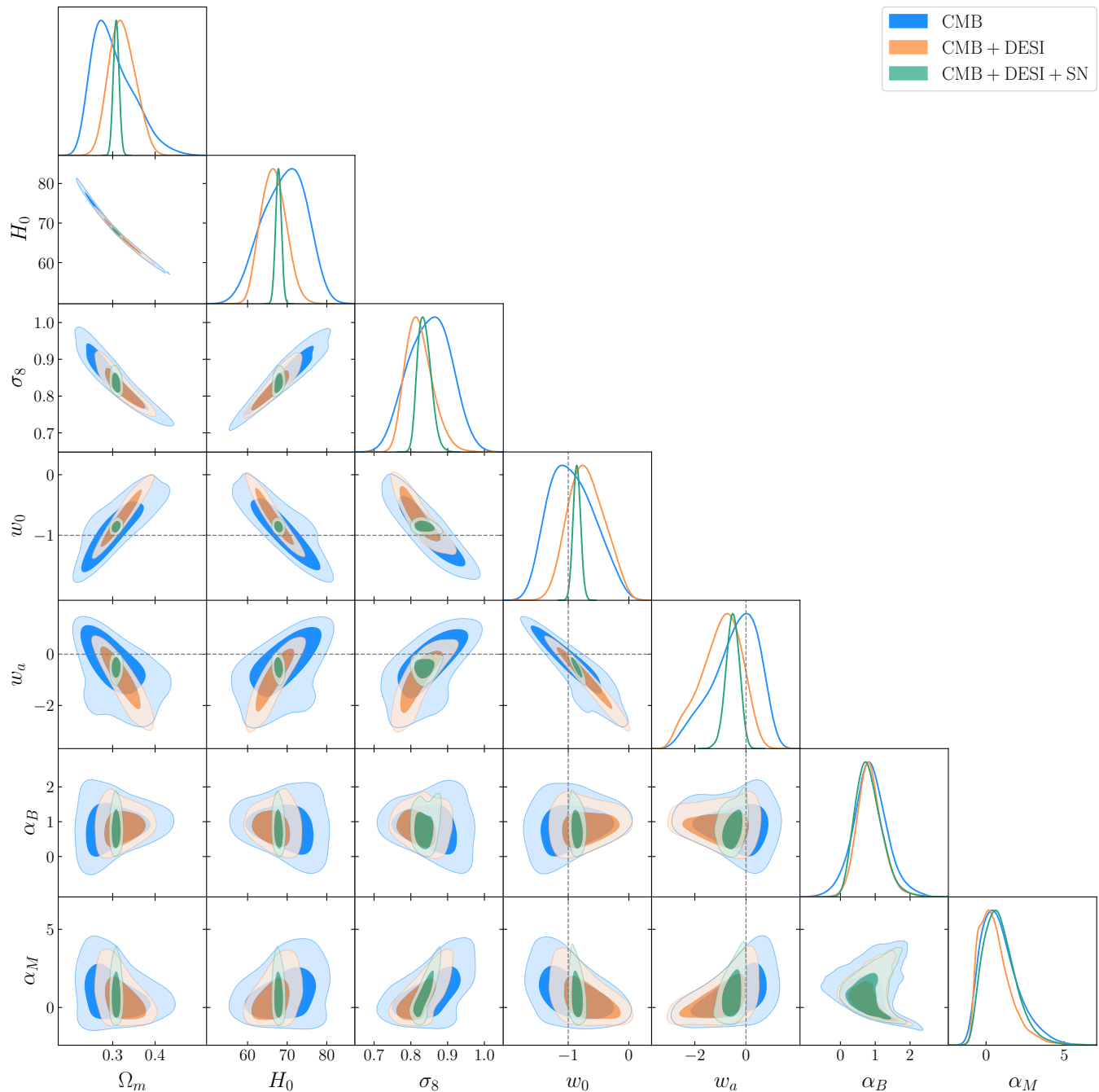


FIG. 5. Posterior distributions of the cosmological parameters in the MG model from the CMB (blue), CMB+DESI (orange) and CMB+DESI+SN (green) datasets.

- Approximation Schemes*, *JCAP* **02** (2020) 008 [1909.01828].
- [16] D. Blas, J. Lesgourgues and T. Tram, *The Cosmic Linear Anisotropy Solving System (CLASS) II: Approximation schemes*, *JCAP* **1107** (2011) 034 [1104.2933].
- [17] A. Gelman and D. B. Rubin, *Inference from Iterative Simulation Using Multiple Sequences*, *Statist. Sci.* **7** (1992) 457.
- [18] PLANCK collaboration, N. Aghanim et al., *Planck 2018 results. VI. Cosmological parameters*, *Astron. Astrophys.* **641** (2020) A6 [1807.06209].
- [19] J. Carron, M. Mirmelstein and A. Lewis, *CMB lensing from Planck PR4 maps*, *JCAP* **09** (2022) 039 [2206.07773].
- [20] ACT collaboration, M. S. Madhavacheril et al., *The Atacama Cosmology Telescope: DR6 Gravitational Lensing Map and Cosmological Parameters*, *Astrophys.*

TABLE III. Constraints on the relevant cosmological parameters. H_0 is measured in units of $\text{km s}^{-1} \text{Mpc}^{-1}$.

Model/Dataset	H_0	Ω_m	σ_8	w_0	w_a	α_B	α_M
$w_0 w_a$ CDM							
CMB+DESI+SN	$67.99^{+0.72}_{-0.74}$	$0.309^{+0.007}_{-0.007}$	$0.818^{+0.010}_{-0.010}$	$-0.821^{+0.063}_{-0.067}$	$-0.76^{+0.31}_{-0.26}$	–	–
CMB+(DESI*+SDSS)+SN	$67.12^{+0.68}_{-0.70}$	$0.318^{+0.007}_{-0.007}$	$0.811^{+0.010}_{-0.010}$	$-0.891^{+0.061}_{-0.063}$	$-0.39^{+0.27}_{-0.23}$	–	–
MG							
CMB	$69.22^{+6.39}_{-5.10}$	$0.302^{+0.032}_{-0.063}$	$0.850^{+0.062}_{-0.059}$	$-0.931^{+0.315}_{-0.478}$	$-0.43^{+1.16}_{-0.64}$	$0.84^{+0.45}_{-0.49}$	$0.87^{+0.73}_{-1.50}$
CMB+DESI	$66.67^{+2.98}_{-3.30}$	$0.321^{+0.028}_{-0.034}$	$0.824^{+0.028}_{-0.043}$	$-0.708^{+0.270}_{-0.338}$	$-0.97^{+0.97}_{-0.62}$	$0.84^{+0.32}_{-0.41}$	$0.62^{+0.54}_{-1.29}$
CMB+DESI+SN	$67.81^{+0.73}_{-0.72}$	$0.308^{+0.007}_{-0.007}$	$0.837^{+0.015}_{-0.021}$	$-0.856^{+0.060}_{-0.064}$	$-0.53^{+0.28}_{-0.26}$	$0.82^{+0.31}_{-0.46}$	$0.88^{+0.75}_{-1.28}$

J. **962** (2024) 113 [2304.05203].

- [21] PLANCK collaboration, Y. Akrami et al., *Planck intermediate results. LVII. Joint Planck LFI and HFI data processing*, *Astron. Astrophys.* **643** (2020) A42 [2007.04997].
- [22] A. J. Ross, L. Samushia, C. Howlett, W. J. Percival, A. Burden and M. Manera, *The clustering of the SDSS DR7 main Galaxy sample – I. A 4 per cent distance measure at $z = 0.15$* , *Mon. Not. Roy. Astron. Soc.* **449** (2015) 835 [1409.3242].
- [23] BOSS collaboration, S. Alam et al., *The clustering of galaxies in the completed SDSS-III Baryon Oscillation Spectroscopic Survey: cosmological analysis of the DR12 galaxy sample*, *Mon. Not. Roy. Astron. Soc.* **470** (2017) 2617 [1607.03155].
- [24] D. Wang, *The Self-Consistency of DESI Analysis and Comment on "Does DESI 2024 Confirm Λ CDM?"*, **2404.13833**.
- [25] EUCLID collaboration, Y. Mellier et al., *Euclid. I. Overview of the Euclid mission*, **2405.13491**.
- [26] E. Bellini and I. Sawicki, *Maximal freedom at minimum cost: linear large-scale structure in general modifications of gravity*, *JCAP* **07** (2014) 050 [1404.3713].
- [27] J. Noller and A. Nicola, *Cosmological parameter constraints for Horndeski scalar-tensor gravity*, *Phys. Rev. D* **99** (2019) 103502 [1811.12928].